

# Neoclassical and Anomalous Transport Analysis of Helical Reactor Plasmas

YAMAZAKI Kozo, MIKHAILOV Mihail<sup>1</sup>, SAKAKIBARA Satoru, OKAMURA Shoichi,  
GARCIA Jeronimo<sup>2</sup>, DIES Javier<sup>2</sup>, FUNABA Hisamichi and AMANO Tsuneo

*National Institute for Fusion Science, Toki 509-5292, Japan*

<sup>1</sup>*Russian Research Centre 'Kurchatov Institute', Moscow, Russia*

<sup>2</sup>*Universitat Politècnica de Catalunya, Barcelona, Spain*

(Received: 9 December 2003 / Accepted: 21 April 2004)

## Abstract

The plasma parameters of the standard LHD (Large Helical Device)-type helical reactor (LHR-S) are estimated using zero-dimensional (zero-D) model with radial parabolic profile correction and 2.0-D (1-D transport / 3-D equilibrium) analysis with neoclassical and anomalous transport models. Zero-dimensional analysis using global confinement scaling laws including “new LHD modified” scaling laws clarifies the required D-T ignition machine scale, magnetic field and confinement improvement factor. The 2.0-D analysis for LHR-S with 450 MW alpha particle power clarifies the feedback burn control behavior and radial profiles of ignited steady-state plasmas. In the case of low-beta inward-shifted configuration and smaller ion anomalous loss, the plasma can be ignited with the major radius  $R$  of  $\sim 15\text{m}$  (4.2 times larger than LHD) and the magnetic field strength  $B$  of  $\sim 5\text{T}$ . The real high beta configuration leads to the increase of effective helical ripple, and the required density regime becomes rather high. If we add the ion anomalous transport, the access to ignition becomes difficult and the thermal instability is found to be excited due to required high-density low-temperature conditions.

## Keywords:

neoclassical transport, confinement scaling laws, effective helical ripple, burn control, helical system, DT ignition, Large Helical Reactor

## 1. Introduction

The helical confinement system has a great advantage of sustaining current-disruption-free steady-state fusion plasmas by external magnetic field. However, in these 3-dimensional (3-D) helical configurations, the magnetic helical ripple might enhance the plasma transport loss.

For understanding fusion plasma dynamics of helical reactors, the analysis on the radial profile distribution is important, and the 3-D equilibrium and 1-D transport should be coupled for reactor predictive simulation. Especially, neoclassical and anomalous transports, beta and density limits, neo-classical radial electric field and magnetic multi-helicity effects are crucial in the prediction of ignited helical reactor plasmas.

Here, we present the results of the simplified zero-D analysis and the detailed 2.0-D analysis including both neoclassical and anomalous losses in helical reactor plasmas

## 2. Transport mode

### 2.1 Neoclassical models

We analyze equilibrium-transport properties using

TOTAL (Toroidal Transport Analysis Linkage Code) simulation code [1] with neoclassical transport including ambipolar electric field and multi-helicity magnetic field effects in addition to semi-empirical anomalous loss or drift turbulent loss models. The total transport coefficient is a summation of asymmetric ripple loss, symmetric neoclassical loss and anomalous loss:

$$\chi = \chi_{rip\nabla T} + \chi_{sym} + \chi_{ano}, \quad (1)$$

where neoclassical thermal loss flux can be written as

$$Q \propto \chi_{rip\nabla n} \nabla n / n + \chi_{rip\nabla T} \nabla T / T - Z E_r / T. \quad (2)$$

Here,  $\chi_{rip\nabla n}$ ,  $\chi_{rip\nabla T}$ ,  $Z$  and  $E_r$  are non-orthogonal diffusivity, orthogonal diffusivity, atomic charge number and radial electric field, respectively. In this paper we used the above  $\chi$  value (Eq. (1)) as a total diffusivity, instead of the effective value ( $\chi_{eff} \propto Q/(\nabla T/T)$ ) used for experimental comparison. The simplified zero-dimensional global plasma prediction for neoclassical model is also carried out.

## 2.2 Anomalous models

As for anomalous transport, we have adopted several models such as empirical model, 6-regime drift wave model, resonant island induced transport model, E×B shear model, and so on. In the present analysis, we focus on the empirical diffusivity model using fixed radial shape factors as

$$\chi \propto (1 + g\rho^m) / f_{imp}^s, \quad (3)$$

where typically  $g = 1$  (flat profile) or 5 (medium), and  $m = 4$ . When the International Stellarator Scaling 1995 (ISS95) is assumed and  $\chi$  is written as a function of temperature instead of global heating power, the exponent  $s$  of the confinement improvement coefficient  $f_{imp}$  should be 2.44. The condition of  $f_{imp-e} = f_{imp-i} = 1$  without neoclassical ripple transport corresponds to the transport predicted by the ISS scaling law. In the reference simulation, the ion improvement coefficient  $f_{imp-i}$  is assumed to be as large as 10.

The anomalous particle diffusion coefficient is assumed as

$$D = C_{ano}\chi_{ano}, \quad C_{ano} = 0.1. \quad (4)$$

The gas puffing and pellet injection fueling models are compared for the density control, which is used for feedback control to get desired fusion power output. As a boundary condition for simulation, the edge density and edge temperature are fixed. The central electron cyclotron heating (ECH) of 200 MW with power deposition width of 30% of plasma minor radius is also assumed for start up and burn control. The alpha particle ripple loss fraction is typically assumed as

$$f_{ripple} = 0.1 + 0.3(1 - \rho^2). \quad (5)$$

## 3. Reactor plasma projection

### 3.1 Zero-dimensional empirical estimation

For zero-dimensional analysis with parabolic radial profiles of density  $n(r) = n_0(1 - (r/a)^2)^{0.5}$  and temperature  $T(r) = T_0(1 - (r/a)^2)^{a_T}$ , where  $a_T$  is 1 or 2, well-known conventional scaling laws can be utilized. Here four conventional global confinement scaling laws based on medium-sized helical experiments are shown: old LHD scaling (LHD), Gyro-Reduced Bohm scaling (GRB), Lackner-Gotardi scaling (LG) and International Stellarator Scaling 1995 (ISS95):

$$\tau_{LHD} = 0.17P^{-0.58}\bar{n}_e^{0.69}B^{0.84}R^{0.75}a^2 \quad (6)$$

$$\tau_{GRB} = 0.25P^{-0.6}\bar{n}_e^{0.6}B^{0.8}R^{0.65}a^{2.4} \quad (7)$$

$$\tau_{LG} = 0.17P^{-0.6}\bar{n}_e^{0.6}B^{0.8}Ra^2\iota_{2/3}^{0.4} \quad (8)$$

$$\tau_{ISS95} = 0.26P^{-0.59}\bar{n}_e^{0.51}B^{0.83}R^{0.65}a^{2.21}\iota_{2/3}^{0.4} \quad (9)$$

Units used here are,  $P$ (MW),  $\bar{n}_e$ ( $10^{20}\text{m}^{-3}$ ),  $B$ (T),  $R$ (m),  $a$ (m), respectively.

Using new plasma kinetic databases in LHD, we reconfirmed that  $\sim 1.5$  times higher confinement time than

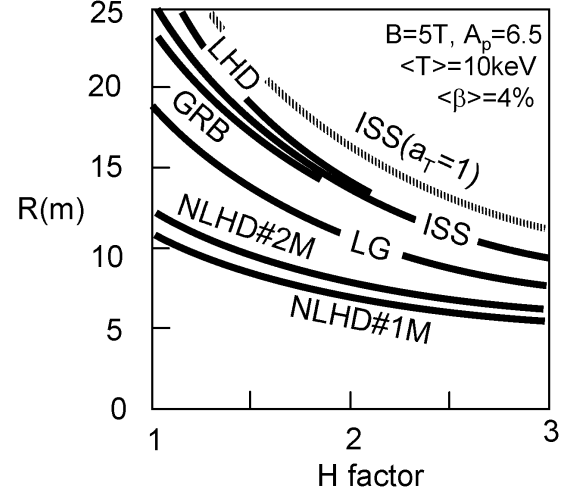


Fig. 1 Effect of confinement improvement factor (H-factor) on the ignition reactor size. One dotted line is for  $\tau(r) \propto (1 - (r/a)^2)^{a_T}$  with  $a_T = 1$ , and Solid curves are for the peaked profile with  $a_T = 2$ .

the ISS95 scaling is obtained (average  $\sim 1.53$ , standard derivative  $\sim 0.46$ ), which corresponds to  $\sim 2$  times of the LHD scaling value (average  $\sim 2.10$ , standard derivative  $\sim 0.86$ ). The reactor plasmas can be extrapolated using these scaling laws with these H-factors [2]. Recently, ‘‘Modified New LHD’’ confinement scaling laws has been derived by the log-linear regression analyses adding LHD high power heating data, [3].

$$\tau_{NLHD-1M} = 0.350P^{-0.59}\bar{n}_e^{0.49}B^{0.95}R^{0.67}a^{2.81}, \quad (10)$$

$$\tau_{NLHD-2M} = 0.127P^{-0.60}\bar{n}_e^{0.49}B^{1.00}R^{1.14}a^{2.20}. \quad (11)$$

The NLHD-1M (root mean square error RMSE = 0.112) is based on experimental data from heliotron-type devices (LHD, ATF, H-E and CHS), and the NLHD-2M (RMSE = 0.126) based on those from all helical devices including W7-AS, W7-A experimental data set. In this analysis we did not include the effect of magnetic rotational transform, because there is a strong correlation between the rotational transform and the aspect ratio. These new global scaling laws suggested the strong gyro-Bohm like feature, which is different from previous conventional scaling laws (Gyo-Bohm like) based on only medium-sized devices (Eqs. (6)–(9)).

Using above global scaling laws, we calculated reactor size with fixed parabolic radial profiles. In the case of ISS scaling laws without confinement improvement, a device with plasma major radius  $R = 30\text{m}$  is required for ignition at  $B = 6\text{T}$  and plasma-aspect-ratio  $A_p = 7$ . In the case of new modified scaling laws,  $R = 10\sim 15\text{m}$  machine is possible without improvement as shown in Fig.1

### 3.2 One-dimensional transport / three-dimensional equilibrium analysis

#### (1) Reference plasma of LHR-S

The one-dimensional transport has been analyzed using TOTAL code [1]. The figure 2 shows the time evolution of ignited helical plasma. In this simulation, the LHR-S (Large

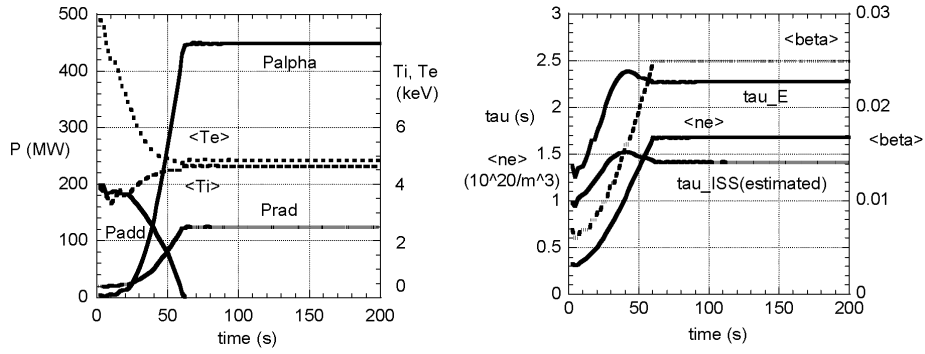
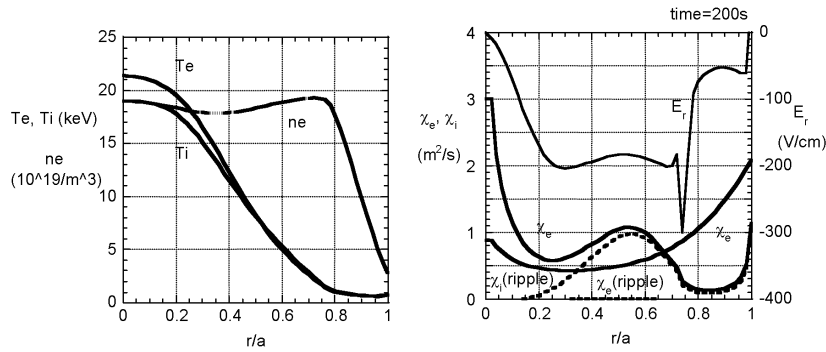


Fig. 2 Time evolution of LHR-S (Large Helical Reactor-Standard) reference plasma.


 Fig. 3 Steady-state radial profiles of ignited LHR-S reference plasma (Fig.1) at  $t = 200$ s. Left: electron and ion temperatures ( $T_e$ ,  $T_i$ ) and electron density ( $n_e$ ) vs.  $r/a$  Right: ripple thermal diffusivity ( $\chi_e(\text{ripple})$ ,  $\chi_i(\text{ripple})$ ), total diffusivity ( $\chi_e$ ,  $\chi_i$ ) and radial electric field ( $E_r$ ).

Helical Reactor-Standard) system [2] having  $R = 15.1$ m,  $B = 5$ T is assumed with  $H$ -factor = 1.6 based on ISS scaling law. The radial profiles of electron anomalous transport coefficient are determined to fit this  $H$ -factor. The target alpha power is 450MW (roughly 1GW-electric). The external heating power is feedback controlled to trace target time evolution. The radiation power is  $\sim 100$ MW in this case.

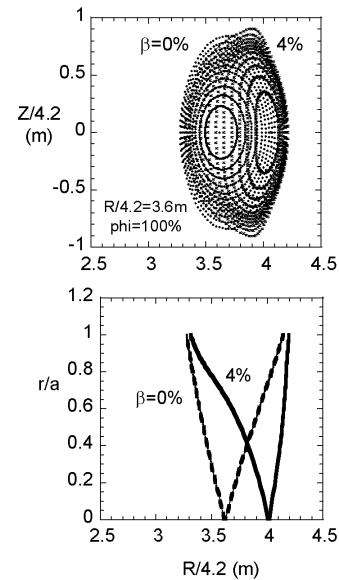
The radial temperature and density profiles are plotted in Fig 3. The electron temperature is mainly determined by anomalous transport in this case. On the other hand, ion temperature strongly depends on the neoclassical ripple loss with negative electric field. These profiles are obtained by the pellet fueling model without anomalous inward particle flow. When the gas-puffing method is used, the required  $H$ -factor is increased due to low density, high temperature core plasmas for same fusion output.

## (2) Effect of radial shape factor of transport coefficient

The central temperature critically depends on the radial  $\chi_{ano}$  profile of transport coefficient. When the heating power deposition is near the center, the central transport coefficient becomes large, which was experimentally verified in the real LHD experiments. According to the simulation analysis, the flat  $\chi_{ano}$ -profile ( $g = 1$ ) requires higher density operation for ignition with 450 MW alpha particle power.

## (3) Effect of magnetic configuration on neoclassical transport

The neoclassical ripple transport is proportional to


 Fig. 4 LHR equilibria with 0% and 4% beta values. Upper: shape of magnetic surfaces, Lower: its position  $r/a$  vs.  $R$ .

$\varepsilon_i^2 \varepsilon_{heff}^{1.5}$  ( $\varepsilon_i$ : inverse aspect ratio,  $\varepsilon_{heff}$ : effective helical ripple). Especially higher beta configuration enhances effective helical ripple in the LHD-type configuration.

Figure 4 shows high-beta magnetic surfaces, and Fig. 5 denotes related effective helical ripples, which are derived using GIOTA code within TOTAL code. The ion ripple loss is enhanced by the finite beta effect ( $\langle\beta\rangle \sim 3\%$ ) and the rather

peaked density profile is required for ignition, as shown in Fig. 6. Here we did not include bootstrap (BS) current effect which might improve neoclassical confinement. The effect of BS current will be clarified in the future.

Here we compare with other configurations CHS-qa [4],  $N = 6$  QP (quasi-poloidal) [5] and  $N = 2$  QP [6]. It should be noted that the neoclassical transport (flux  $\Gamma \propto \epsilon_t^2 \epsilon_{heff}^{3/2}$  without radial electric field) strongly depends on magnetic configurations and plasma beta values. The detailed comparisons between LHR (LHD Reactor), QAR (Quasi-Axisymmetric Reactor) and QPR (Quasi-Poloidal Reactor)

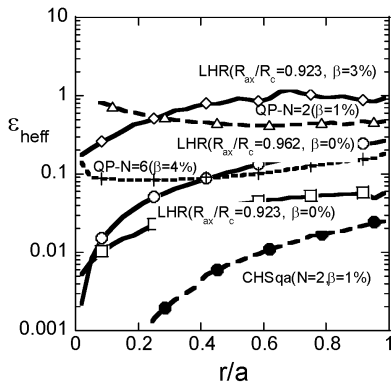


Fig. 5 Effective helical ripple for various magnetic configurations.

transport properties with neoclassical and anomalous loss models including radial electric field will be discussed in the future.

#### (4) Effect of ion anomalous transport

As for anomalous loss, we considered the electron and ion improvement coefficients,  $f_{impe}$  and  $f_{impi}$ , based on the ISS95 scaling laws. In the reference design, we assume electron anomaly exists ( $f_{impe} = 2.0-4.0$ ) but ion anomalous loss is small ( $f_{impi} > 10$ ). When the ion anomaly factor is same as electron's one, it is more difficult to reach ignition. Figure 7 shows the time evolution of the produced alpha power and plasma parameters. The higher density is required and the plasma becomes thermally unstable when both density and heating power are feedback controlled. The higher confinement improvement factor should be assumed for reaching ignition.

### 4. Summary

We can summarize this paper as follows;

- (1) The reactor plasma of the Standard LHD-type Reactor (LHR-S) is projected using zero-dimensional (0-D) analysis with profile correction and 2.0-D (1-D transport / 3-D equilibrium) analysis with neoclassical and anomalous loss models.
- (2) Zero-dimensional analysis using global scaling including "New LHD Modified" confinement scaling laws clarifies the required major radius and magnetic field for DT ignition.

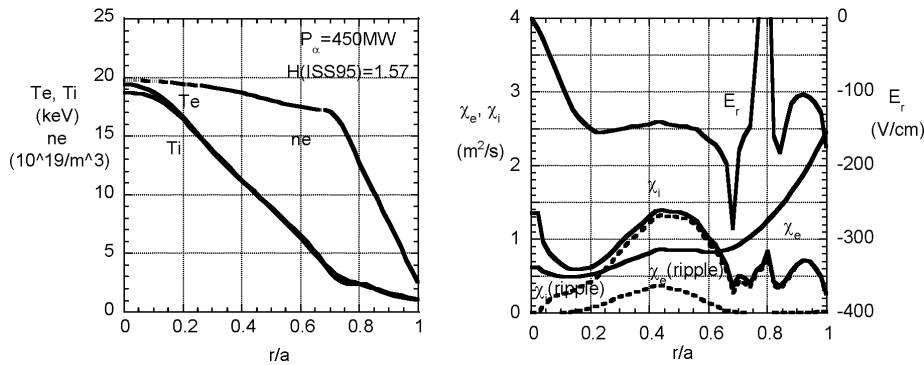


Fig. 6 Ignited plasma profile in LHR-S using 3% beta equilibrium.

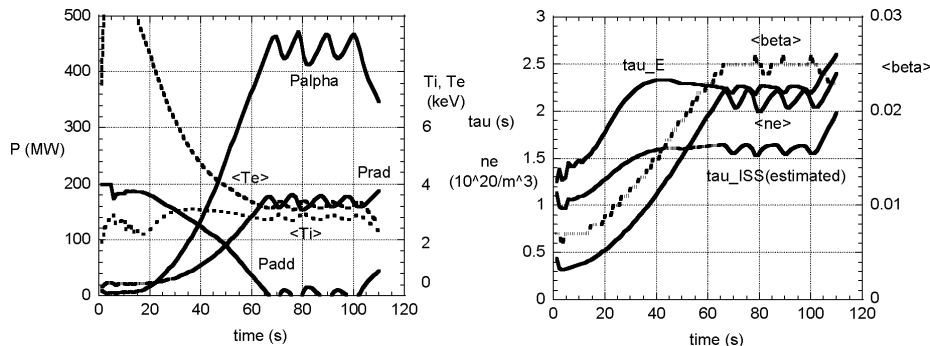


Fig. 7 Time evolution of LHR-S plasma including ion anomalous loss.

- (3) The 2.0-D analysis for LHR-S with 450 MW alpha particle power clarifies the feedback burn control behavior and radial profiles of ignited plasmas.
- (4) In the case of the low-beta inward-shifted configuration and no ion anomalous loss, the plasma can be ignited for  $R \sim 15\text{m}$  ( $\sim 4$  times larger than LHD) and  $B \sim 5\text{T}$ .
- (5) The high beta configuration leads to the increase of effective helical ripple in LHR-S, and the higher density and higher confinement improvement factor are required.
- (6) If we include the ion anomalous transport same as electron, the ignition becomes difficult and the thermal instability is excited due to the lower plasma temperature regime.

## References

- [1] K. Yamazaki and T. Amano, Nucl. Fusion **32**, 633 (1992).
- [2] K. Yamazaki *et al.*, “*Helical Reactor Design Studies Based on New Confinement Scalings*”, 18th IAEA Fusion Energy Conference IAEA-CN-77/FTP 2/12 (Italy, Sorrento, 2000).
- [3] K. Yamazaki *et al.*, “Global and Local Confinement Scaling Laws of NBI-Heated Gas-Puffing Plasmas on LHD” EPS-2003 (St Petersburg, July 7-11, 2003) P-3.16.
- [4] S. Okamura *et al.*, Nucl. Fusion **41**, 1865 (2001).
- [5] M. Mikhailov *et al.*, Nucl. Fusion **42**, L23 (2002).
- [6] M. Samitov *et al.*, this conference.